Efficient femtosecond optical parametric oscillator with dual-wavelength operation

Liang Xu,[1,*] Xin Zhong,[2] Jiangfeng Zhu,[1] Hainian Han,[2,3] and Zhiyi Wei[2,4]

[1]School of Technical Physics, Xidian University, Xi'an 710071, China

[2]Beijing National Laboratory for Condensed Matter Physics, Institute of Physics, Chinese Academy of Sciences, Beijing 100190, China

[3]e-mail: hnhan@iphy.ac.cn

[4]e-mail: zywei@iphy.ac.cn

*Corresponding author: liang_xu@stu.xidian.edu.cn

Received October 28, 2011; revised February 26, 2012; accepted March 5, 2012; posted March 6, 2012 (Doc. ID 157132); published April 23, 2012

We demonstrated on a synchronously pumped femtosecond optical parametric oscillator with dual-signal-wavelength operation. Our results showed that the dual-wavelength oscillation is not determined by the net-zero dispersion but rather by the balance of phase matching and group-velocity mismatching caused by the nonlinear crystal between the two signals. With a MgO-doped periodically poled lithium niobate as the nonlinear crystal, total signal power up to 530 mW was obtained by using a 2.6 W femtosecond Ti:sapphire laser at the central wavelength of 808 nm as the pump source, corresponding to a conversion efficiency of 20.4%. By slightly adjusting the cavity length, the signal wavelength can be broadly tuned from 1001 to 1438 nm and the dual-wavelength tuning range is from 1001 to 1204 nm.

OCIS codes: 190.4970, 190.4410, 320.7110, 320.7090.

Since the first demonstration of a femtosecond optical parametric oscillator (OPO) in 1989 [1], an ultrafast OPO system was recognized as a superior tunable laser source that can cover the wavelengths from ultraviolet to mid-infrared spectral range [2–4] for many applications, such as time-resolved spectroscopy, optical signal processing, remote sensing, laser medicine, coherent light interactions, etc. Compared with the conventional birefringent phase-matching technique using KTP, KTA, etc. [5,6] for nonlinear parametric processes, the quasi-phase-matching (QPM) [7] technique shows clear advantages due to the large nonlinear coefficient. Up to now, periodically poled crystals have been widely used in QPM OPOs. For instance, Andres *et al.* obtained signal power of 310 mW by using a periodically poled lithium niobate (PPLN) crystal as the gain medium in a femtosecond OPO [8], which was synchronously pumped by a Kerr-lens-mode-locking (KLM) Ti:sapphire laser. Similar signal power up to 345 mW was also demonstrated by Bhupathiraju *et al.* from a femtosecond OPO with periodically poled stoichiometric $LiTaO_3$ crystal as the nonlinear gain medium [9].

In particular, a femtosecond OPO operating at dual wavelength has potential advantages in differential frequency generation THz generation [10], wavelength-division-multiplex communications, waveform synthesis [11], coherent control [12], etc. To realize the dual-wavelength operation, a common method is to design the femtosecond OPO operating close to the net-zero-dispersion region [13], where these two pulses operating at different group-velocity dispersion regions have the same round trip time delay. Thus both pulses are synchronized to the pump pulse and show phase coherence between each other, which can be controlled by, for example, cavity-length tuning, a promising application in frequency comb [14].

In this paper, we report on new experimental research on a synchronously pumped femtosecond OPO with a MgO-doped PPLN crystal operating at dual-wavelength mode. Experimental results show that the dual-wavelength oscillation is not determined by the cavity dispersion but rather by the balance of phase matching and group-velocity mismatching between the two signals. Total signal output power as high as 530 mW was generated, which operates at dual wavelength with center wavelengths at 1024.8 and 1195.3 nm, respectively, when pumped by a 2.6 W femtosecond Ti:sapphire oscillator, corresponding to a conversion efficiency of 20.4%. By slightly adjusting the cavity length, the signal wavelength can be broadly tuned from 1001 to 1438 nm and the dual-wavelength tuning range is from 1001 to 1204 nm.

The experimental layout is shown in Fig. 1. A self-built high-power KLM Ti:sapphire oscillator operating at a repetition rate of 76 MHz is used as the pump source for the OPO, which is capable of 2.6 W average power at the central wavelength of 808 nm with an FWHM of 15 nm. Autocorrelation measurement indicates the typical pulse duration is 117 fs. In the OPO cavity, M1 is a flat mirror that is mounted on a translation stage. Precisely adjusting the translation stage will enable control of the cavity length for synchronous pumping. M2 and M3 are concave

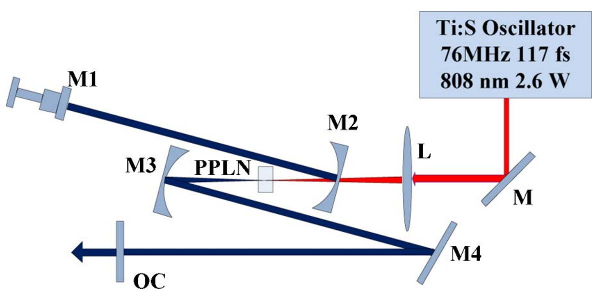

Fig. 1. (Color online) Schematic diagram of the experimental layout. L, lens with 75 mm focal length; M1, plane mirror mounted on a translation stage; M2 and M3, concave mirrors with ROC of 10 cm; M4, folding mirror; OC, output coupler.

0146-9592/12/091436-03$15.00/0

mirrors with radii of curvature (ROC) of 10 cm. All mirrors are coated with high reflection ($R > 99.8\%$) over 1.00–1.45 μm wavelength range. The output coupler (OC) has a transmission rate of 2.5% in the 1.0–1.45 μm wavelength range. Based on the simulation of efficient parametric process within the above wavelength range, we used a 5% mol MgO-doped PPLN crystal with a poling period of 22.12 μm as the nonlinear gain medium, which is cut with a 2 mm optical path and 3 mm × 1 mm optical aperture. The cavity length of the OPO is set to be half that of the Ti:sapphire oscillator, to make the OPO running at a repetition rate of 152 MHz.

For a fixed poled period ($\Lambda = 22.12$ μm) and the same pump power, different pump wavelengths will result in different conversion efficiencies and output powers. In our experiment, the highest output power was obtained when the pump wavelength was centered at 808 nm. Under 2.6 W pump power, the highest output power of signal was 530 mW, which operates at dual wavelength with center wavelengths at 1024.8 and 1195.3 nm, respectively, and corresponds to an optical-to-optical conversion efficiency of 20.4%. Considering the energy conversion in the idler branch, the calculated total photon conversion efficiency is 30.7% based on the photon conservation law. Signal wavelength is tuned by adjusting the translation stage of M1 to slightly vary the cavity length. We find there are two signal oscillation regions, single-wavelength oscillation and dual-wavelength oscillation, by shortening the cavity length. Firstly, the OPO operates at single-wavelength oscillation from 1438 to 1204 nm. Then, dual-wavelength oscillation occurs at 1001 and 1204 nm. The separation between the dual wavelength gets closer by shortening the cavity length and finally merges as a single wave at 1150 nm. Further shortening the cavity length will cause too big a cavity length mismatch, and as a result the signal disappears. We believe the single-wavelength oscillation is due to the mirror coating that all mirrors besides the OC have, with high reflection from 1.00 to 1.45 μm, so that the other wavelength is suppressed. For the case of the two signals close to merge in the dual-wavelength oscillation region, the two pulses get closer both in the frequency domain and in the time domain. As a result, the oscillator becomes unstable due to the mode competition between the two signals. Except for this case, the OPO is stable for both the single-wavelength and dual-wavelength oscillation. Figure 2 shows the evolution process of the dual-wavelength emission spectra by shorting the cavity length. In the single-wavelength operation region, we measured the pulse duration with an intensity autocorrelator (FR-103MN, Femtochrome Research, Inc.). For the signal centered at 1257 nm, the FWHM width of the autocorrelation trace shows that the pulse duration is 342 fs, assuming a sech^2 pulse shape, as shown in Fig. 3(a). The time bandwidth product is calculated to be 0.726, indicating there is big residual chirp in the cavity. This is apparent because we introduce no chirp compensation element in the cavity. Figure 3(b) shows the intensity autocorrelation trace of the signal when the OPO is operating at the dual-wavelength region, which is measured when the two signals are centered at 1027 and 1191 nm, respectively, as indicated in Fig. 2(b). The interference fringes shown in Fig. 3(b) clearly prove the synchronism and coherence between the two pulses, while the decreased contrast in the intensity autocorrelation fringes indicates that there is group-velocity mismatch (GVM) between the two signals.

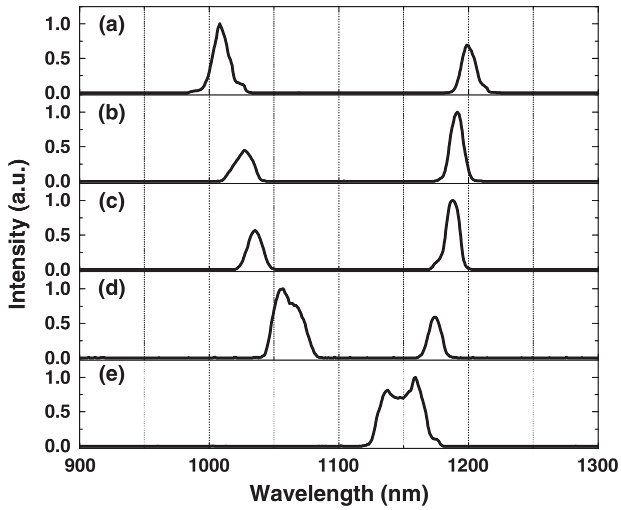

Fig. 2. Evolution of the dual-wavelength spectra while the cavity length was shortened. In (b), the two wavelengths are centered at 1027 and 1191 nm, respectively.

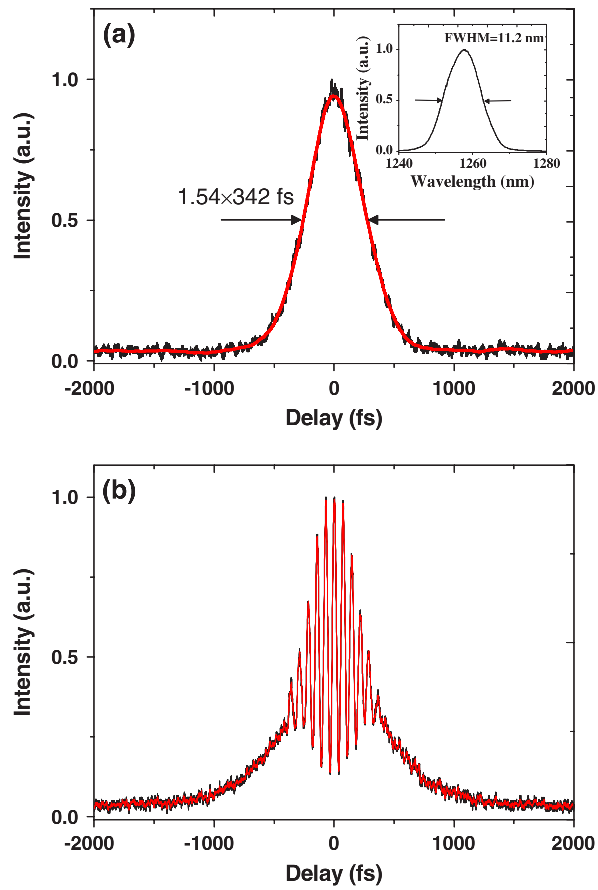

Fig. 3. (Color online) Intensity autocorrelation trace of the signal (a) when operating at the single-wavelength region at 1257 nm and (b) in the dual-wavelength region at 1024.8 and 1195.3 nm, respectively. The red curve is the smoothed one of the measurement.

The dual-wavelength operation in our femtosecond OPO is in good agreement with that in the picosecond region [15]. Since the dominant dispersive element is the 2 mm long PPLN crystal, and there is no dispersion compensation element in the OPO cavity, the dual-wavelength pulses suffer from group-velocity dispersion (GVD) due to the PPLN crystal, and as a result they do not operate around the 0 GVD region [14]. In the experiment, the signal-pulse duration is three times longer than that of the pump pulse, so it is easy to get overlap between them. In addition, the 2 mm long PPLN crystal introduces a large GVM between the signal and pump, which is 296 fs and 414 fs for the two signals centered at 1024.8 and 1195.3 nm (where the oscillator has the highest output power), respectively. It indicates a GVM of 118 fs between the two signal pulses, which means only one signal pulse can overlap well with the pump pulse. Under these special conditions, one of the signal pulses (the red one) is well phase matched with the pump pulse but suffers from larger GVM, while the other one (the blue one) benefits by a better overlap with the pump but has a worse phase-matching condition. Consequently, the net gain of the two signals is comparable, and thus the dual-wavelength operation occurs. Beyond this specific wavelength range, the balance between the phase matching and group-velocity mismatching breaks, and thus dual-wavelength oscillation disappears and evolves to single-wavelength oscillation.

In conclusion, we have realized an efficient synchronously pumped femtosecond optical parametric oscillator with dual-wavelength operation. With a 5% mol MgO-doped PPLN crystal as the gain medium, total signal power up to 530 mW was obtained when pumped by a 2.6 W mode-locked femtosecond Ti:sapphire laser. It is shown in our experiment that the dual-wavelength operation can be broadly tuned from 1001 to 1209 nm by slightly adjusting the cavity length; beyond this cavity-length tuning range, the singly resonant signal wavelength can be further tuned to 1438 nm. Dual-wavelength operation benefits from the balance of phase matching and group-velocity mismatching between the two signals. The synchronism and coherence between the coresonant pulses makes this OPO an attractive and promising tool for many applications in ultrafast optics.

We thank the helpful discussion with Qing Wang, Dehua Li, and Hao Teng. This work is partly supported by the National Natural Science Foundation of China under grant 10874237 and the Knowledge Innovation Program of the Chinese Academy of Sciences (No. KJCX2-YW-N36).

References

1. D. C. Edelstein, E. S. Wachman, and C. L. Tang, Appl. Phys. Lett. **54**, 1728 (1989).
2. M. Ghotbi, A. Esteban-Martin, and M. Ebrahim-Zadeh, Opt. Lett. **33**, 345 (2008).
3. A. Esteban-Martin, V. Ramaiah-Badarla, V. Petrov, and M. Ebrahim-Zadeh, Opt. Lett. **36**, 1671 (2011).
4. F. Adler, K. C. Cossel, M. J. Thorpe, I. Hartl, M. E. Fermann, and J. Ye, Opt. Lett. **34**, 1330 (2009).
5. W. S. Pelouch, P. E. Powers, and C. L. Tang, Opt. Lett. **17**, 1070 (1992).
6. D. T. Reid, M. Ebrahim-Zadeh, and W. Sibbett, Opt. Lett. **20**, 55 (1995).
7. K. J. Han, D. W. Jang, J. H. Kim, C. K. Min, T. H. Joo, Y. S. Lim, D. H. Lee, and K. J. Yee, Opt. Express **16**, 5299 (2008).
8. T. Andres, P. Haag, S. Zelt, J. P. Meyn, A. Borsutzky, R. Beigang, and R. Wallenstein, Appl. Phys. B **76**, 241 (2003).
9. K. V. Bhupathiraju, A. D. Seymour, and F. Ganikhanov, Opt. Lett. **34**, 2093 (2009).
10. T. Taniuchi and H. Nakanishi, J. Appl. Phys. **95**, 7588 (2004).
11. S. W. Huang, G. Cirmi, J. Moses, K. H. Hong, S. Bhardwaj, J. R. Birge, L. J. Chen, E. Li, B. J. Eggleton, G. Cerullo, and F. X. Kartner, Nat. Photon. **5**, 475 (2011).
12. Y. Kobayashi, H. Takada, M. Kakehata, and K. Torizuka, Opt. Lett. **28**, 1377 (2003).
13. K. C. Burr, C. L. Tang, M. A. Arbore, and M. M. Fejer, Appl. Phys. Lett. **70**, 3341 (1997).
14. J. H. Sun, B. J. S. Gale, and D. T. Reid, Opt. Lett. **31**, 2021 (2006).
15. L. Tartara, Opt. Lett. **32**, 1105 (2007).